IOP Conf. Series: Journal of Physics: Conf. Series **1455** (2020) 012005 doi:10.1088/1742-6596/1455/1/012005

Large-Scale Fabrication of Optically Active Plasmonic Arrays via Displacement Talbot Lithography

Eugeniu Balaur[a,b,*], Catherine Sadatnajafi[a,b], Brian Abbey[a,b]

[a]Australian Research Council Centre of Excellence for Advanced Molecular Imaging, Victoria, Australia
[b]Department of Chemistry and Physics, La Trobe Institute for Molecular Science (LIMS), La Trobe University, Victoria, Australia

Email: E.Balaur@latrobe.edu.au

Abstract : Periodic nanoapertures fabricated in thin metal films exhibit a range of interesting properties in the presence of electromagnetic waves including phenomena such as extraordinary optical transmission (EOT). Fundamentally, these effects are mediated by plasmons and have been shown to have a vast range of applications, including, colour filtering, chemical sensing, and as components in solar cells. In the majority of cases, the high spatial resolution required for precise fabrication of these structures is limited to direct writing techniques such as Focused Ion Beam (FIB) and Electron beam lithography (EBL), which only cover relatively small, micron-sized, areas. In this article, we describe and demonstrate the fabrication of plasmonically active devices in the visible range using Displacement Talbot Lithography (DTL). This method allows nanometre-resolution photolithography to be performed over very large areas (whole wafers) without any significant degradation in quality. We present experimental results for a range of different structures including periodic, aperiodic and hexagonal configurations in silver films.
Keywords: Talbot lithography;periodic nanostructures; plasmonic materials; metallic films.

1. Introduction

Extraordinary Optical Transmission (EOT) in the context of plasmonic metamaterials is a phenomenon which has attracted much attention in recent years. The characteristics of EOT include a considerable increase in the optical transmission from structures which are smaller than the wavelength of the incident electromagnetic field compared to the classically predicted value [1]. One of the most common types of metamaterial comprises a highly-periodic arrays of nanoapertures fabricated in a thin metallic film [2, 3]. The propagation and the behavior of electromagnetic waves passing through these structures can be readily understood using the theory of plasmons in which an electromagnetic wave couples with the oscillations of free electrons within the thin film [4]. Due to the plasmonic nature of such metamaterials they have been exploited in a wide variety of contexts including color filtering [5, 6], chemical sensing [7-9] and, components in solar cells [10].

The fabrication of periodic, high-quality, arrays of sub-wavelength nanoapertures has typically been achieved via Focused Ion Beam (FIB) lithography techniques [11]. This technique allows for precise and versatile prototyping in a range of different materials, from metals and semiconductors all the way through to dielectrics [12]. Due to its dual beam capabilities (ion and electron), a fast inspection after the milling process is readily possible using FIB which helps with optimization of the fabrication parameters. One of the major drawbacks of FIB lithography, however, is the slow patterning rate, which severely limits the practical achievable working field-of-view (usually ~ 100 × 100 um). For high-resolution sub-100 nm fabrication, low ion beam currents (~ 100 pA) are often used, which further limits the feasibility of patterning structures on a large scale. As a result of these limitations alternative patterning techniques have been explored, such as Electron Beam Lithography (EBL), nanoimprinting and high-end photolithography. All of these techniques can produce large scale patterned areas with nanometer resolution, however, each has their drawbacks. For example, EBL is still very slow when patterning large areas and is limited to single wafer processing. Nanoimprinting meanwhile has the potential to pattern large areas, however, it suffers from stamp degradation and particulate contamination due to the contact mode of fabrication. High-end Photolithography employs commercial grade steppers, which are expensive, elaborate and are still limited to a fixed patterning field (~26x33 mm) for a single exposure. The growing need for fast, low-cost, and easy-to-use nanoscale patterning of large-scale areas has driven the development of a range of alternate photolithographic techniques.

One of the most recent emerging techniques capable of fulfilling these requirements is Displacement Talbot lithography (DTL) [13]. DTL uses a combination of self-imaging and Talbot sub-imaging to produce nanometer-size periodic patterns with a spatial resolution well-beyond the working wavelength of the source [13].

Here we report a simple, yet versatile procedure, for fabricating functional plasmonic devices over the whole 4" wafers which employs the DTL and e-beam evaporation techniques. To demonstrate this approach, we have fabricated a range of periodic, aperiodic and hexagonal arrays of patterns. The influence of deposition rates and metal film thickness is discussed.

2. Materials and Methods

Glass wafers (4" diameter) were first spin-coated with a back-antireflection coating to avoid parasitic reflections, a ~500 nm-thick i-line sensitive photoresist was thin spin-coated onto the active surface. The DTL exposure was performed using a monochromatic UV beam with the substrate-to-mask distance in the range of 30–50 μm, and a displacement in the range 1.3 μm to 2.7 μm depending on the grating period. To achieve the necessary dose, the total exposure time per wafer took 2-3 min. Masks of 800 and 1000 nm grating periodicity were used to produce the rectangular array, and 600 nm periodicity for the hexagonal array fabrication. To obtain the aperiodic structures, a double exposure method was employed, in which the grating mask was rotated by 90° between the two exposures.

Upon development, the wafers were coated with silver (Ag) films primed with a 3 nm germanium (Ge) seed layer via electron-beam evaporation with varying deposition rates. Following deposition, a lift-off procedure was performed in an ultra-sonicating bath for 5 min in acetone and isopropanol respectively to remove the unbound metal film and the photoresist. The wafers were then rinsed with isopropanol, ultra-pure water, and blow-dried using a nitrogen stream. This process is summarised in Figure 1 (a). SEM images were collected using anFEI NovaNanoSEM.Transmission spectra were acquired on a Nikon Ti-U inverted optical microscope with a 20× objective, using a spectrometer (Ocean Optics QE *Pro*) with a diffraction grating of 600 lines/mm. All spectra were normalized with respect to the white-field illumination through the bare substrate.

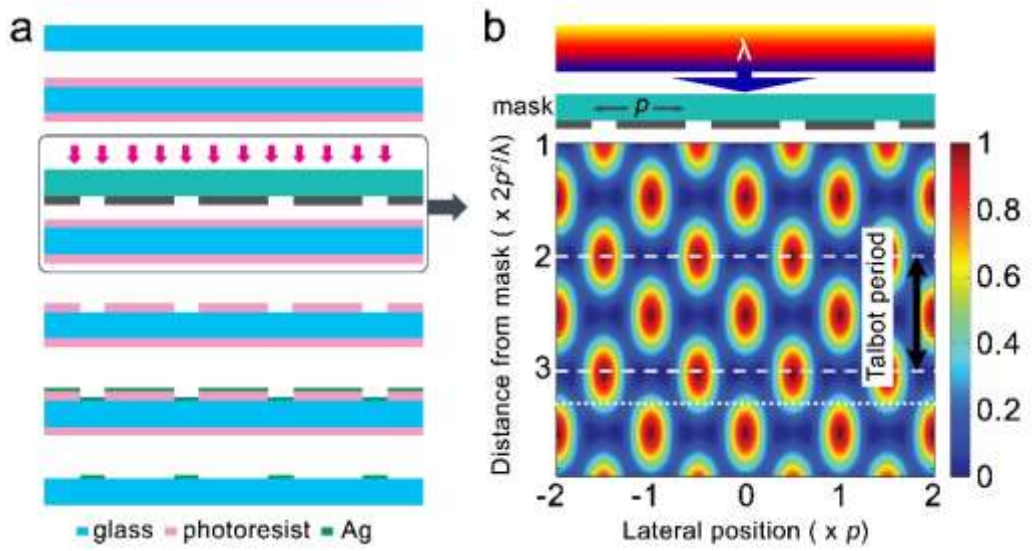

Fig. 1. (a) Process flow; (b) Simulated EM intensity distribution after a linear grating.

Figure 1 (b) shows two self-images (marked with white dashed lines) located at a distance $x2p^2/\lambda\mu m$ from the grating. The thin white dotted horizontal linedenotes the position of the Talbot sub-image, which has twice the frequency of the original grating.

3. Results and Discussions

Figure 2 shows representative SEM images of a circular aperture array after lift-off with high-magnification insets illustrating the highquality of the patterns. The inset in Figure 2 (a) shows an SEM image of a FIB cross-section through the diameter of the aperture showing the quartz substrate, Ge, and Ag layers. In order to achieve a clean cut through the layers, Pt/C e-beam induced deposition was used to cover the device prior to milling. The cross-section of these structures reveals that the beveled profile of the patterns is around 86° and that no metal residues are present around the aperture. Patterns of different configurations were fabricated using a range of periodicities and symmetries. The 400 nm square arrays reveal circular apertures with ~195 nm diameter. The corresponding spectra and optical images (insets in the spectral data) show that there is little effect from linearly polarized light. Small changes in the spectra and corresponding optical images are attributed to minor imperfections during the fabrication process; changes in the nm range lead to significant changes in the position of plasmonic resonant peaks (REF). The 400 × 500 nm rectangular arrays reveal elliptical apertures with ~195 × 225 nm radiuses. This effect is caused by a different grating period on the mask used to expose the photoresist. The 400 nm lines result in a smaller exposed field compared to the 500 nm lines, as shown in Fig. 1 (b). As the resulting patterns are obtained by double exposure from two masks (with 800 and 1000 nm grating periods), the resulting profile after development becomes elliptical. The corresponding spectral data and optical images demonstrate how these aperiodic structures behave under polarized light. The main plasmonic resonant peaks change as the polarization vector of the incident light varies from 0^0 to 90^0. The 600 nm hexagonal arrays exhibit circular apertures with ~195 nm radius. These arrays were produced in a single exposure with no aperiodicity, therefore there is almost no sensitivity to polarization as demonstrated by the spectral and optical data. We observe that increasing the periodicity of the arrays leads to both a red shift of the resonant peaks and a reduction in the total transmitted intensity due to the decrease of overall ratio of aperture area and the bare film.

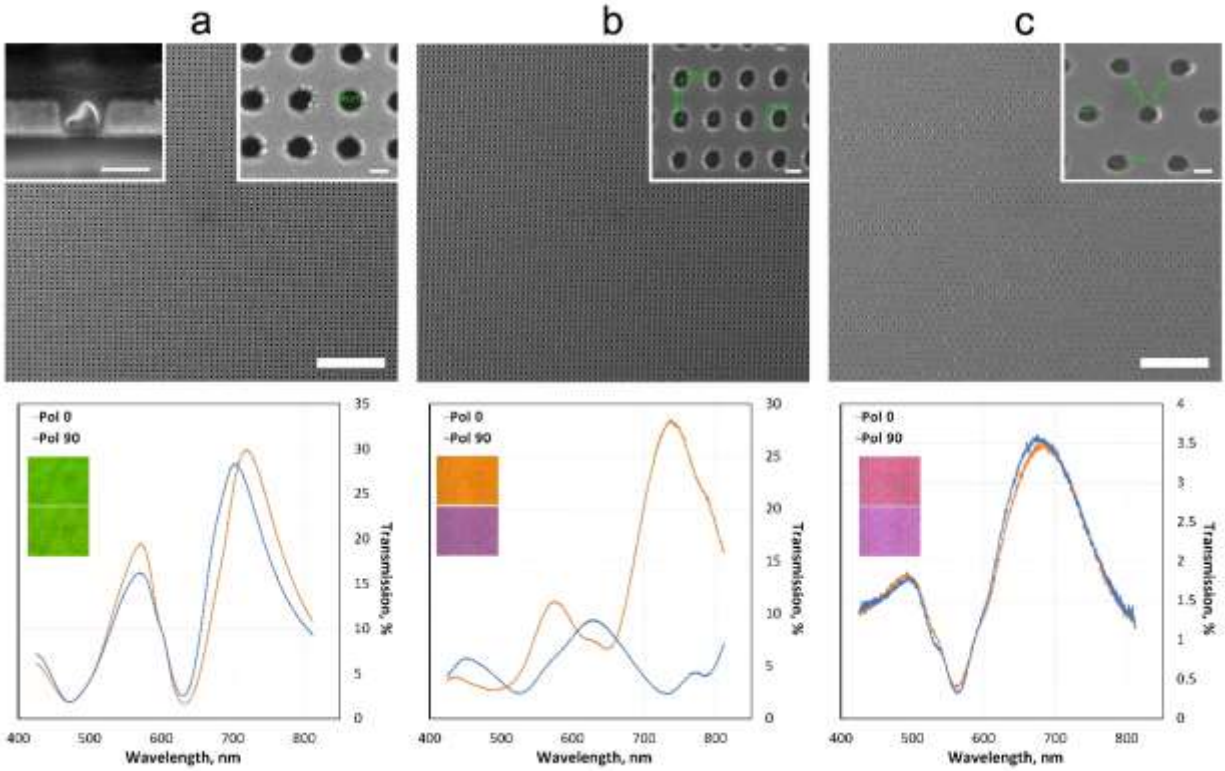

Fig. 2. SEM images and corresponding transmission spectra for: (a) Square array with 400 nm period; (b) aperiodic rectangular array of 400 × 500 nm period; (c) periodic hexagonal array of 600 nm period, the scale bars are 5 um and 200 nm for the main images and insets respectively.

In order to characterize the effect on the FWHM of the resonant peaks we next studied the influence of varying the film thickness and the deposition rate of the Ag film. Figure 3 (a) and (b) show transmission spectral data for a 400 × 500 nm rectangular array fabricated in 150 and 200 nm thick Ag films respectively.

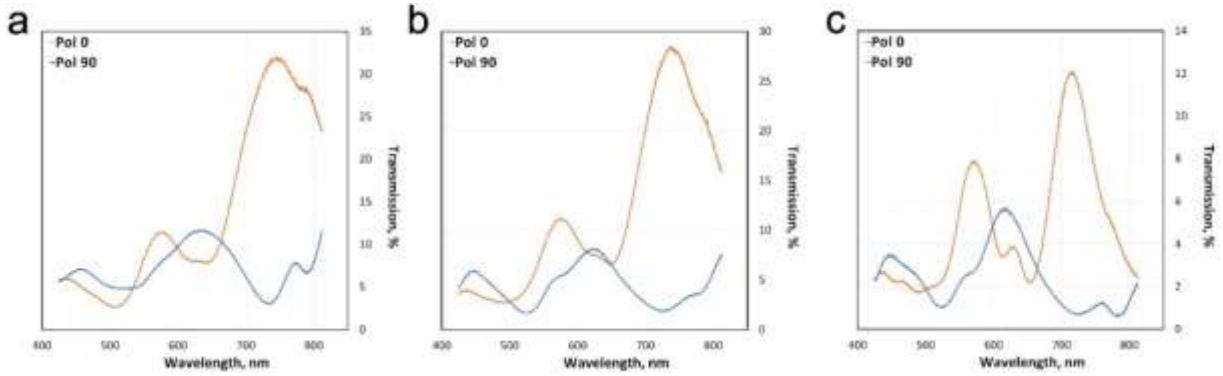

Fig. 3. Transmission spectra fora rectangular array of 400x500 nm period: (a) in 150 nm Ag films deposited at 0.5 A/s rate; (b) in 200 nm Ag films deposited at 0.5 A/s rate; (c) in 200 nm Ag films deposited at 50 A/s rate.

Increasing the film thickness was found to lead to better-defined resonant peaks, although at the expense of a slight decrease of the transmitted intensity. Recently (REF), it was demonstrated that it is possible to obtain metal films of much higher quality for plasmonic applications by using very high deposition rates (> 50 Å/s). Figure 3 (c) shows transmission spectral data for a 400 × 500 nm rectangular array fabricated in 200 nm Ag films deposited using a 50 Å/s deposition rate. We note that the resonant peaks are much better defined and the appearance of the satellite peaks (Wood anomalies[14]) are clearly distinguishable.

4. Conclusions

We have described and demonstrated a simple method of fabrication of large-scale plasmonic structures exhibiting the EOT effect using the Displacement Talbot Lithography method. Employing this technique, it is possible to achieve various structures including square, rectangular, and hexagonal arrays. The optical output can be tuned by varying the periodicity of the mask used for the exposure. By increasing the thickness of the metal films, the transmission properties are found to be significantly improved. Furthermore, by using very high deposition rates, we observe that much higher quality structures can be obtained. It is envisaged that these findings will be significant for a wide-range of applications based on metamaterials including color filtering and chemical sensing applications.

Acknowledgements

The authors acknowledge the support of the Australian Research Council through the Centre of Excellence in Advanced Molecular Imaging. This work was performed in part at the Melbourne Centre for Nanofabrication (MCN) in the Victorian Node of the Australian National Fabrication Facility (ANFF).

References

[1] T. W. Ebbesen, H. J. Lezec, H. F. Ghaemi, T. Thio, and P. A. Wolff, Nature 391 (1998) 667-669.
[2] E. Balaur, C. Sadatnajafi, S. S. Kou, J. Lin, and B. Abbey, Scientific Reports 6 (2016) 28062.
[3] D. Langley, E. Balaur, C. Sadatnajafi, and B. Abbey, SPIE BioPhotonics Australasia 10013 (2016) 1001338.
[4] L. Martin-Moreno, F. J. Garcia-Vidal, H. J. Lezec, K. M. Pellerin, T. Thio, J. B. Pendry, and T. W. Ebbesen, Phys. Rev. Lett. 86 (2001) 1114-1117.
[5] E. Balaur, C. Sadatnajafi, D. Langley, and B. Abbey, SPIE BioPhotonics Australasia 10013 (2016) 100132F.
[6] R. R. Unnithan, M. Sun, X. He, E. Balaur, A. Minovich, D. N. Neshev, E. Skafidas, and A. Roberts, Materials 10 (2017) 383.
[7] D. P. Langley, E. Balaur, Y. Hwang, C. Sadatnajafi, and B. Abbey, Adv Funct Mater 28 (2018) 1704842.

[8] J. Homola, S. S. Yee, and G. Gauglitz, Sensors and Actuators B: Chemical 54 (1999) 3-15.
[9] J. N. Anker, W. P. Hall, O. Lyandres, N. C. Shah, J. Zhao, and R. P. Van Duyne, Nat. Mater. 7 (2008) 442-453.
[10] J. Gwamuri, D. Ö. Güney, and J. M. Pearce, Advances in Plasmonic Light Trapping in Thin-Film Solar Photovoltaic Devices, Scrivener Publishing LLC., 2013, 402-269.
[11] L. A. Giannuzzi, Introduction to Focused Ion Beams, Springer US, New York, 2005.
[12] S. Jahani, and Z. Jacob, Nature Nanotechnology 11 (2016) 23-26.
[13] H. H. Solak, C. Dais, and F. Clube, Optics Express 19 (2011) 10686.
[14] Y. W. Jiang, L. D. C. Tzuang, Y. H. Ye, Y. T. Wu, M. W. Tsai, C. Y. Chen, and S. C. Lee, Optics Express 17 (2009) 2631-2637.